Molecular Cell, Vol. 5, 545–555, March, 2000, Copyright ©2000 by Cell Press

Asymmetry in the PPARγ/RXRα Crystal Structure Reveals the Molecular Basis of Heterodimerization among Nuclear Receptors

Robert T. Gampe, Jr., Valerie G. Montana, Millard H. Lambert, Aaron B. Miller, Randy K. Bledsoe, Michael V. Milburn, Steven A. Kliewer, Timothy M. Willson, and H. Eric Xu*
Glaxo Wellcome Research and Development
Research Triangle Park, North Carolina 27709

Summary

The nuclear receptor PPARγ/RXRα heterodimer regulates glucose and lipid homeostasis and is the target for the antidiabetic drugs GI262570 and the thiazolidinediones (TZDs). We report the crystal structures of the PPARγ and RXRα LBDs complexed to the RXR ligand 9-*cis*-retinoic acid (9cRA), the PPARγ agonist rosiglitazone or GI262570, and coactivator peptides. The PPARγ/RXRα heterodimer is asymmetric, with each LBD deviated ~10° from the C2 symmetry, allowing the PPARγ AF-2 helix to interact with helices 7 and 10 of RXRα. The heterodimer interface is composed of conserved motifs in PPARγ and RXRα that form a coiled coil along helix 10 with additional charge interactions from helices 7 and 9. The structures provide a molecular understanding of the ability of RXR to heterodimerize with many nuclear receptors and of the permissive activation of the PPARγ/RXRα heterodimer by 9cRA.

Introduction

Peroxisome proliferator-activated receptor γ (PPARγ) is a member of the nuclear receptor superfamily of ligand-activated transcription factors that serves as a key regulator of adipocyte differentiation and glucose homeostasis (Schoonjans et al., 1997; Willson and Wahli, 1997; Spiegelman, 1998; Willson et al., 2000). PPARγ is the molecular target for the thiazolidinediones (TZDs), a new class of antidiabetic drugs that includes troglitazone (Rezulin), rosiglitazone (Avandia), and pioglitazone (Actos). These drugs, which sensitize tissues to the actions of insulin, lower glucose and fatty acid levels in patients with type 2 diabetes. PPARγ agonists may also have utility in the treatment of other disease states, including inflammation and cancer (Kliewer and Willson, 1998). We have recently reported a novel chemical class of PPARγ ligands, exemplified by GI262570, that were optimized for binding to human PPARγ (Henke et al., 1998; Brown et al., 1999). These tyrosine-based compounds are two to three orders of magnitude more potent than the glitazones currently in clinical use.

PPARγ binds to DNA as a heterodimer with the retinoid X receptors (RXRs), receptors for the vitamin A metabolite 9-*cis*-retinoic acid (9cRA) (Kliewer et al., 1994; Tontonoz et al., 1994). The three RXR subtypes (α, β, γ) bind to DNA and activate transcription in response to 9cRA as homodimers. However, the RXRs also serve as common heterodimeric partners for ~15 of the class 1 nuclear receptors, including the retinoic acid, thyroid hormone, and vitamin D receptors (Mangelsdorf and Evans, 1995). Thus, RXRs are essential components of multiple endocrine signaling pathways. Some of the RXR heterodimers, including those formed between the PPARs and RXRs, are "permissive" in that they can be activated by 9cRA. RXRs also form permissive heterodimers with LXR and FXR, nuclear receptors for oxysterols and bile acids, respectively. The dual modulation of these permissive heterodimers by either cognate ligand provides an additional level of regulation of these hormone signaling pathways (Mangelsdorf and Evans, 1995).

The effects of hormones on PPARγ, RXR, and other nuclear receptors are mediated through the ligand-binding domain (LBD), a conserved region of ~250 amino acids in the C-terminal half of the receptor (Weatherman et al., 1999). In addition to its role in hormone binding, the LBD also contains dimerization and transactivation functions, including the transcriptional activation function 2 (AF-2). Upon hormone binding, the LBD undergoes a conformational change, most notably in the AF-2 domain. These conformational changes result in the displacement of corepressor proteins, such as NCoR and SMRT, that inhibit transcription and the recruitment of coactivator proteins, such as p160 and DRIP/TRAP, family members that are involved in transcriptional activation (Freedman, 1999).

Our understanding at the molecular level of how nuclear receptor ligands exert their effects has been dramatically enhanced by the elucidation of the crystal structures of the apo- and/or ligand-bound LBDs of several nuclear receptors (Bourguet et al., 1995; Renaud et al., 1995; Wagner et al., 1995; Brzozowski et al., 1997; Klaholz et al., 1998; Nolte et al., 1998; Williams and Sigler, 1998; Xu et al., 1999). These structures have revealed a common fold among LBDs, consisting of an antiparallel α-helical sandwich of 11–13 helices. The helices fold to form a hydrophobic cavity into which the ligand can bind. The AF-2 domain is contained within the C-terminal α helix. Two recent cocrystal structures of either PPARγ (Nolte et al., 1998) or estrogen receptor α (Shiau et al., 1998) bound to ligands and complexed with peptides derived from coactivator proteins revealed that the precise positioning of the AF-2 helix is an important determinant in coactivator interactions. Interestingly, the AF-2 helix has been alternately determined as protruding into solution in the apo-RXRα structure (Bourguet et al., 1995) or packed against the body of the receptor in the apo-PPARγ (Nolte et al., 1998; Uppenberg et al., 1998) and apo-PPARδ (Xu et al., 1999) crystal structures. Comparison of the apo-RXRα structure with other ligand-bound nuclear receptor structures suggested a mousetrap model in which the AF-2 helix undergoes a dramatic conformational change in response to ligand. In contrast, comparison of the apo-

*To whom correspondence should be addressed (e-mail: ex11957@glaxowellcome.com).

Table 1. Statistics of Crystallographic Data and Refinement

Heterodimer Complexes	9cRA-Rosiglitazone	9cRA-GI262570
Space group	P21	P212121
Resolution (Å)	20.0–2.1	20.0–2.1
Unique reflections (N)	64,772	25,483
Completeness (%)	94.9	98.8
I/σ (last shell)	25.7 (2.6)	21.2 (2.1)
R_{sym}[a] (%)	4.9	9.4
Refinement statistics		
R factor[b] (%) (2σ)	24.2	23.9
R-free (%) (2σ)	28.8	26.8
r.m.s.d. bond		
Lengths (Å)	0.010	0.012
r.m.s.d. bond		
Angles (degrees)	1.543	1.606
Number of H_2O molecules	450	133
Total non hydrogen atoms	8883	4345

r.m.s.d. is the root mean square deviation from ideal geometry.
[a] $R_{sym} = \Sigma|Iavg - Ii|/\Sigma Ii$
[b] $R_{factor} = \Sigma|F_P - F_{Pcalc}|/\Sigma F_P$, where F_P and F_{pcalc} are observed and calculated structure factors, R_{free} is calculated from a randomly chosen 10% of reflections that have never been used in refinement, and R_{factor} is calculated for the remaining 90% of reflections.

and ligand-bound PPARγ or PPARδ structures suggested a much more subtle change in the position of the AF-2 helix in response to ligand binding, which leads to a stabilized charge clamp for coactivator recruitment.

Despite extensive biochemical and structural studies, the molecular basis of RXR heterodimerization and permissiveness has remained unclear. In this paper, we describe crystal structures of the liganded PPARγ/RXRα heterodimer. We report the structures of two six component complexes, which include the PPARγ and RXRα LBDs, 9cRA, either rosiglitazone or the novel PPARγ agonist GI262570, and peptides derived from the coactivator SRC-1. These structures define a general motif for RXR heterodimerization and provide insights into the molecular mechanism for permissiveness. Moreover, they provide a framework for the rational design of high-affinity ligands targeted against the PPARγ/RXRα complex for use in the treatment of type 2 diabetes and other diseases.

Results

Structure Determination

The PPARγ/RXRα heterodimer was crystallized in the presence of an excess of 9cRA, rosiglitazone, and a peptide derived from the coactivator SRC-1, containing a single LxxLL motif. Purification of the coexpressed PPARγ/RXRα heterodimer and addition of the SRC-1 peptide were critical for crystallization (see Experimental Procedures). Crystals of this complex diffracted to 2.1 Å and occupied the P21 space group, with two heterodimer complexes in each asymmetry unit. In parallel experiments, crystals were grown with the tyrosine analog GI262570 in place of rosiglitazone. These crystals also diffracted to 2.1 Å but occupied the P212121 space group, with one heterodimer complex in each asymmetry unit. The structures were determined by the molecular replacement method with the PPARγ/SRC-1 structure (Nolte et al., 1998) and a 9cRA-bound RXRα model (A. B. M., unpublished data) as the searching models. Electron density maps calculated with phases from the molecular replacement solutions showed clear features for the respective ligands, the LxxLL motifs of the SRC-1 peptides, and each LBD, except for helix 2 of RXRα and the loop between H2′ and H3 of PPARγ. The statistics of data sets and structures are summarized in Table 1.

Global Structure of the PPARγ/RXRα Heterodimer

The structure of the PPARγ/RXRα heterodimer complex contains six components: the two receptor LBDs, their two respective ligands, and two SRC-1 peptides (Figure 1). The complex is butterfly shaped, with both LBDs adopting the conserved "helical sandwich" fold previously reported for other ligand-bound nuclear receptors (front view in Figure 1). PPARγ contains 13 α helices and 4 short β strands, and the gross structure resembles the PPARγ homodimer. RXRα is composed of 11 α helices and 2 short β strands, but the ligand-bound structure shows large conformational changes in H3, H10, and the AF-2 helix compared with the apo-RXR structure (Bourguet et al., 1995).

The PPARγ and RXRα ligands occupy their respective ligand-binding cavities, which lie in the lower half of the LBDs. Both PPARγ and RXRα are in the active configuration, such that the AF-2 helix is folded against the main body of their respective LBDs. The AF-2 helix, together with H3 and H4, form a hydrophobic groove into which the coactivator peptide binds. Two SRC-1 peptides are present in each heterodimer complex where residues 630–639 of the peptide are ordered in the RXRα complex and residues 628–643 are ordered in the PPARγ complex. The overall structure of the coactivator-binding site and the docking modes of the SRC-1 peptide are similar to those observed in the other nuclear receptor coactivator structures (Figure 1) (Nolte et al., 1998; Shiau et al., 1998). In each receptor, the coactivator-binding site is a groove formed by H3, H3′, and H4 at the top and by the AF-2 helix at the bottom. The floor and the sides of this groove are composed of hydrophobic residues. The SRC-1 peptide contains a two-turn amphipathic α helix, which is positioned over the hydrophobic groove between the charge clamp, formed by the lysine

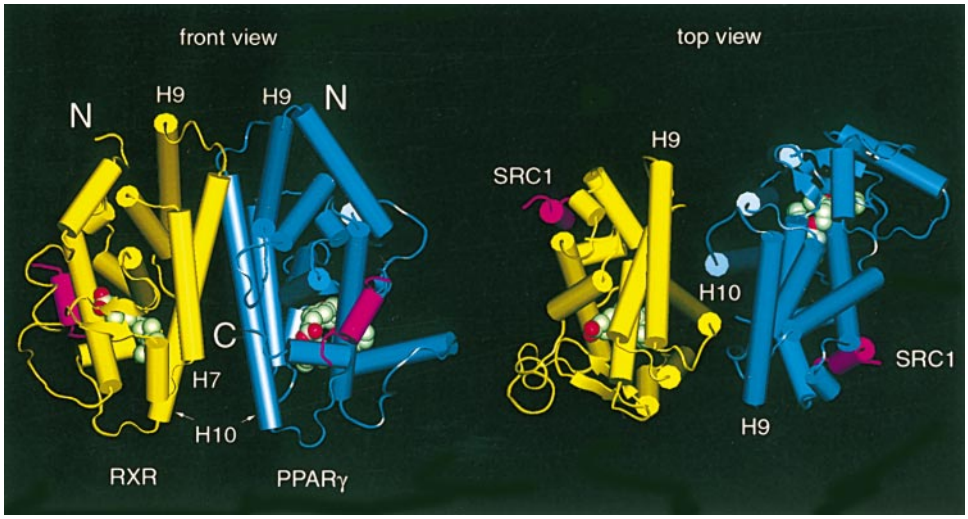

Figure 1. Overall Structure of the PPARγ/RXRα Heterodimer Complex

The front and top views of the PPARγ/RXRα heterodimer complex are presented in solid rendering (α helices in cylinders, and β strands in arrows). RXR is colored in yellow, PPARγ in blue, and the two SRC-1 peptides in purple. The two compounds (9cRA and GI262570) are shown in space-filling representation with carbon, oxygen, and nitrogen atoms depicted in green, red, and blue, respectively.

and the glutamate residues, as seen in the PPARγ homodimer structure with SRC-1 (Nolte et al., 1998).

The Heterodimer Interface

The PPARγ/RXRα interface is asymmetric where the PPARγ LBD is rotated ~10° from the C2 symmetry axis of the RXR LBD. The interface is comprised of an intricate network of hydrophobic and polar interactions mediated by H7, H9, and H10 and the loop between H8 and H9 of both receptors (Table 2). The complementarity of the hydrophobic and charged residues in the heterodimer interface is evident from examination of the electrostatic surface of each receptor (Figure 2). The core hydrophobic interactions between the two receptors are further stabilized by basic and acidic surfaces, which lie on alternate sides of the C2 symmetry axis for PPARγ and RXRα and effectively neutralize each other in the heterodimer. The majority of the heterodimerization interactions are mediated through H10 of both receptors (Table 2; Figure 3a). The N-terminal halves of H10 form a parallel coiled-coil structure, which contributes 10 of the 18 residues that are involved in heterodimerization (Figure 3a). This dimerization interface, which involves residues 432–447 in PPARγ and residues 415–434 from RXRα, is composed of complimentary hydrophobic amino acids. In addition to H10, residues L414 of PPARγ and Y397 of RXR on H9 contribute to the heterodimer interface. Finally, residues from H7, H9, and the loop between H8 and H9 are involved in the formation of hydrogen bonds that further increase the specificity and stability of the dimer interface.

Table 2. Interactions in the RXRα/PPARγ Dimer Interface

Non polar interactions		Polar Interactions	
RXRα	PPARγ	RXRα	PPARγ
(H9) Y397	A433 (H10)	(H7) K356	E407 (H9)
(H10) F415	A433 (H10)	(H7) K356	G395 (L8)
(H10) A416	L414 (H9)	(H7) D379	K438 (H10)
(H10) A416	F432 (H10)	(H7) D379	D441 (H10)
(H10) A416	L436 (H10)	(H9) E390	K434 (H10)
(H10) L419	L436 (H10)	(H9) E394	K434 (H10)
(H10) L420	L414 (H10)	(H9) E401	Q430 (H9)
(H10) L420	L436 (H10)	(H9) R393	D441 (H10)
(H10) L420	Q437 (H10)	(H9) Y397	Q437 (H10)
(H10) L420	M439 (H10)	(H10) K417	E407 (H9)
(H10) L422	T440 (H10)	(H10) R421	E407 (H9)
(H10) P423	T440 (H10)	(H10) R421	D396 (L8)
(H10) P423	M439 (H10)	(H10) R426	Q444 (H10)
(H10) S427	Q444 (H10)	(H10) S427	R443 (H10)
(H10) L430	Q444 (H10)	(H10) K431	Y477 (AF2)
(H10) L430	T447 (H10)		
(H7) E352	P398 (L8)		
(H7) R348	Y477 (AF2)		

Residues involved in dimerization are listed along with the secondary structures. The intermolecular interactions are grouped into polar and nonpolar interactions. The nonpolar interactions include Van der Waals contacts and hydrophobic interactions with a distance cutoff of 4.5 Å, and the polar interactions include charged interactions (5.5 Å cutoff) and hydrogen bonds (4.0 Å cutoff).

Members of the nuclear receptor subfamily 2, which includes RXR, COUP-TF, and HNF4 (Nuclear Receptors Nomenclature Committee, 1999), are unique in having a glutamic acid residue (E352 in RXRα) in the middle of H7 that we designate the "E insert." Close examination of the 9cRA-RXRα portion of the heterodimer structure reveals an unwinding of H7 that is absent in the published apo-RXRα structure (Bourguet et al., 1995). The unwinding of H7 by the E insert initiates an intricate series of charge-driven interactions along the heterodimer interface. The E insert rotates K356 one residue around H7 of RXR, which places it close to a negatively charged region at E407 on the surface of PPARγ (Figure 3b). E352 also makes a salt bridge with R348 on H7, holding this residue in close proximity to K431 on H10 of RXRα. An unexpected consequence of these interactions is the formation of a salt bridge between K431 of

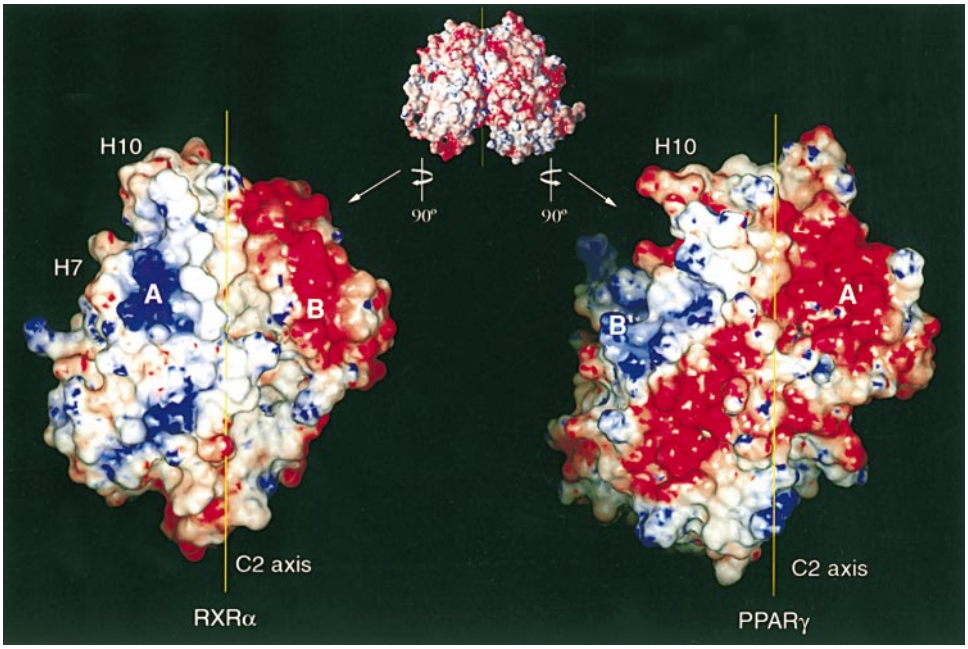

Figure 2. The PPARγ/RXRα Heterodimer Interface

Molecular surface representations of RXRα and PPARγ are colored according to electronic potentials ranging from −6 to +6 kcal/mol/e. The color spectrum includes red for negative charge, white for neutral, and blue for positive charge. The approximate C2 symmetry axis between the two LBDs is indicated, and the regions of charge complementarity are labeled as "A" and "B" in RXR and "A′" and "B′" in PPARγ.

RXRα and the free carboxylate of Y477 in PPARγ (Figure 3b). This salt bridge is further reinforced by a packing interaction between the side chains of Y477 and R348. Thus, E352 of RXRα forms an intradimer salt bridge with R348, which facilitates an interdimer salt bridge between K431 of RXRα and the C-terminal residue of the PPARγ. These salt bridges stabilize the PPARγ AF-2 helix in a position that facilitates the recruitment of coactivators. Notably, the corresponding interaction between the RXRα AF-2 helix and H10 of PPARγ was not observed. These charge-driven interactions, which are asymmetric with respect to the heterodimer, suggest a structural basis for the permissiveness of the PPARγ/RXRα complex.

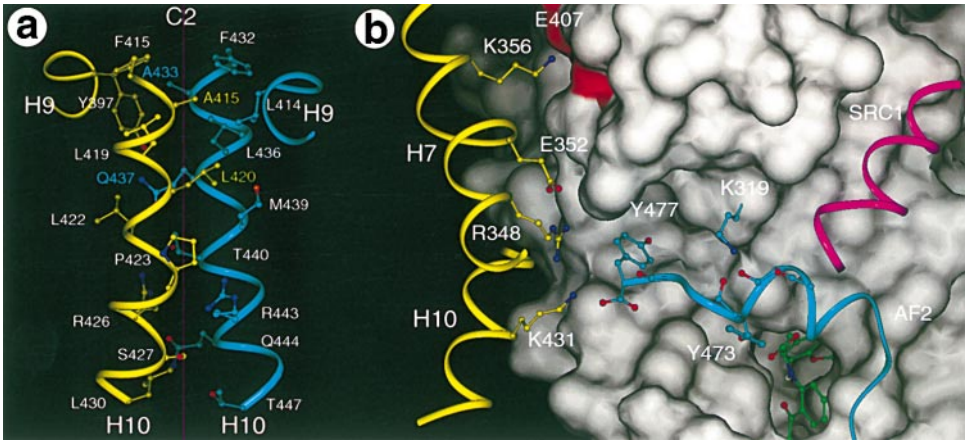

Figure 3. Interactions between RXRα and PPARγ

(a) Intermolecular interactions mediated by helices 10 of RXRα and PPARγ. Key residues that form the core hydrophobic interface of the parallel coiled coil are labeled, along with the C2 axis of symmetry.

(b) Interactions between the PPARγ AF-2 helix and RXRα. Helices 7 and 10 of RXRα are shown in yellow, with residues that form key charge interactions with PPARγ indicated, including the E insert, E352. The surface of PPARγ is shown in gray, with the AF-2 helix of PPARγ indicated in cyan. PPARγ residues Y477, the C-terminal residue that interacts with K431 and R348 of RXRα; K319, which caps the C-terminal carbonyls of the AF-2 helix; and Y473, which interacts with the PPARγ ligands, are indicated. The LxxLL motif of SRC-1 is shown in magenta.

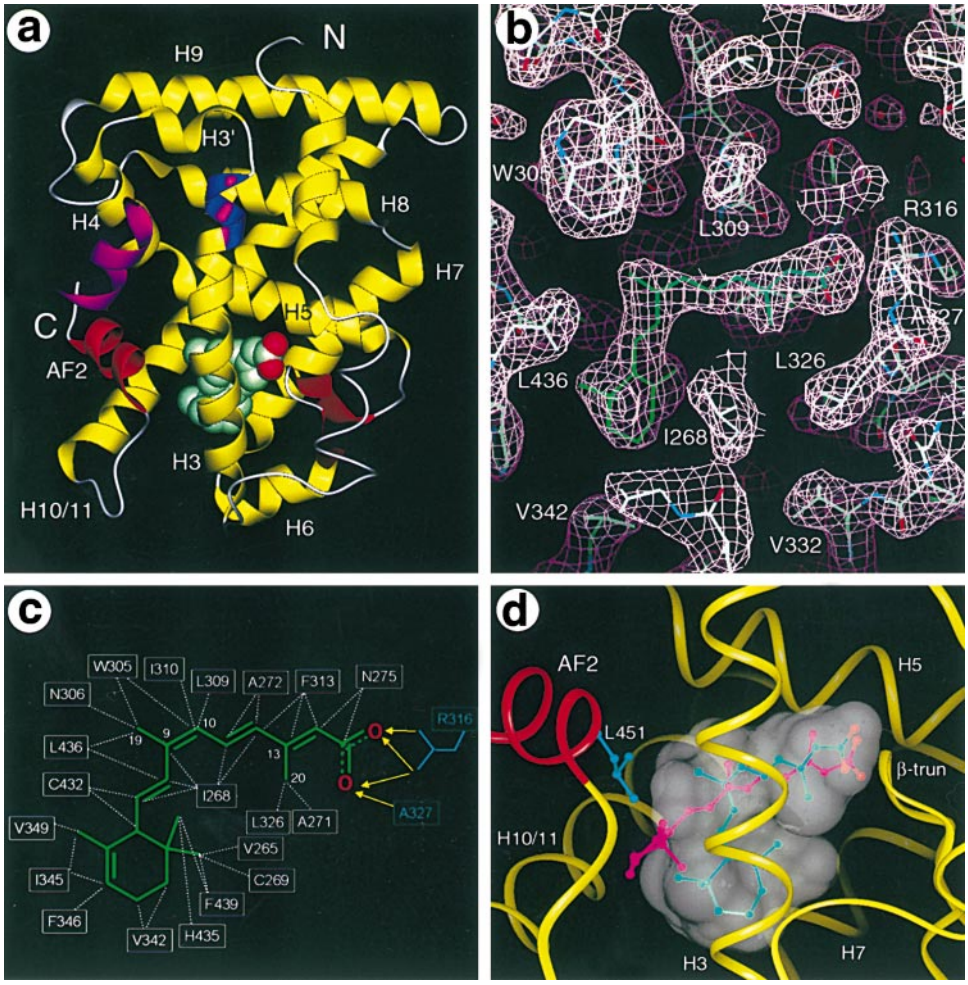

Figure 4. Recognition of 9cRA by RXRα

(a) Ribbon drawings of the RXRα LBD bound to the SRC-1 LxxLL motif (magenta) and 9cRA. The AF-2 helix (red) and residues surrounding the conserved H3 lysine, which comprise the charge clamp, are indicated.

(b) Electron density map for 9cRA molecules. The map was calculated in the absence of the compound with 2Fo-Fc coefficients and contoured at 1.0 σ. The 9cRA carbons are shown in green.

(c) Interactions between 9cRA and RXRα. Residues involved in hydrogen bond interactions and hydrophobic interactions are indicated in blue and white, respectively.

(d) Docking conformation of 9cRA (green carbon atoms) in the RXRα ligand-binding pocket (gray surface). atRA (purple carbon atoms) from the atRA/RARγ structure is superimposed on the 9cRA/RXRα structure.

Binding of 9cRA to RXR

The PPARγ/RXRα crystal structures provide a detailed description of ligand–receptor interactions in a ligand-bound RXRα complex (Figure 4a). Similar to the all-*trans*-retinoic acid– (atRA-) bound structure of RAR (Renaud et al., 1995), 9cRA is completely buried within the bottom half of the RXRα LBD (Figure 4a). The enclosed 9cRA-binding pocket is composed of residues from H3, H4, H5, H7, H10, and the β turn and adopts a sharp turn at residue W305 (Figure 4b). The total volume of this L-shaped pocket is ~470 Å^3, and 9cRA occupies ~75% of the pocket in a low-energy conformation.

The high-affinity binding of 9cRA to RXR can be accounted for by its complimentary hydrophobic and electrostatic interactions with the protein (Figure 4c). The carboxylate of 9cRA makes three hydrogen bonds with the side chain of R316 and one with the backbone amide of A327. A similar hydrogen bond network is seen with the carboxylate of atRA in its complex with RAR (Renaud et al., 1995), demonstrating the conservation of the acid-binding motif across both families of nuclear retinoid receptors. The remaining part of 9cRA is hydrophobic and makes a series of Van der Waals interactions with the ligand pocket. The triene portion of 9cRA makes interactions with I268, A272, N275, L309, I310, and F313. The C20 methyl group contacts A271 and L326, and the C19 methyl group contacts W305, L436, and the methylene of N306. The β ionone ring sits in a pocket that is formed by V265, C269 from H3, V342, I345, F346, V349 from H7, C432, H435, and L436 from H10 (Figure 4c). The structure is supported by observations that mutations in residues I310, F313, R316, A327, and L436 reduce the binding affinity of 9cRA for RXR (Wurtz et al., 1996; Peet et al., 1998).

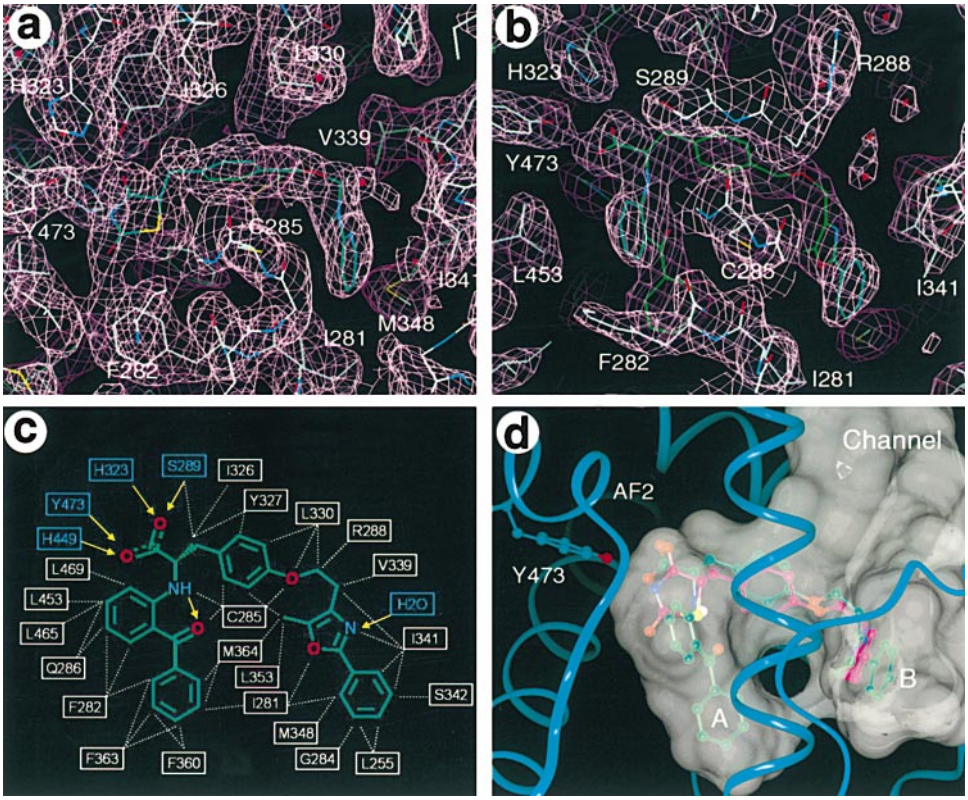

Figure 5. Recognition of Rosiglitazone and GI262570 by PPARγ

(a and b) Electron density maps for the rosiglitazone (a) and GI262570 (b) molecules within the PPARγ pocket. The maps were calculated in the absence of the compounds with 2Fo-Fc coefficients and contoured at 1.0 σ.

(c) Interactions between GI262570 and PPARγ. Residues involved in hydrogen bond interactions and hydrophobic interactions are indicated in blue and white, respectively.

(d) Comparisons of the docking modes of GI262570 (green carbons) and rosiglitazone (purple carbons) in the PPARγ ligand-binding pocket (gray surface). The pockets that are not filled by rosiglitazone but are occupied by the benzophenyl group ("A") and the benzyl tail ("B") of GI262570 are indicated, as is the Y473 residue from the AF-2 helix.

Interactions of 9cRA with the AF-2 helix of RXRα were not observed. In fact, at their closest, 9cRA and the AF-2 helix are >6 Å apart. How then does binding of 9cRA activate RXR? When bound to RXRα, the β ionone ring of 9cRA interacts with hydrophobic residues from H3 and H10/11 (Figure 4c), stabilizing these two helices in a wedge-shaped conformation. In this conformation, L436, F437, and F439 from H10/11; C269, A272, L276, and F277 from H3; and W305 from H5 form a large hydrophobic pocket. The AF-2 helix is held in the active configuration by the docking of hydrophobic residues F450, L451, M452, M454, and L455 into this hydrophobic pocket. The C-terminal carbonyl of the AF-2 helix is capped by R302 in H4, which is conserved as a positively charged residue among many nuclear receptors. Thus, the binding of 9cRA to RXRα initiates a series of intramolecular interactions that stabilize the AF-2 helix in a position that permits coactivator recruitment.

RXR shows high-affinity binding to 9cRA but not to atRA (Heyman et al., 1992; Levin et al., 1992). By comparison, RAR binds to both 9cRA and atRA. Differences in the shape of the ligand-binding pockets of RXR and RAR dictate this ligand selectivity. RAR has a relatively linear I-shaped pocket with a bulge on one end that can easily accommodate either 9cRA or atRA in low-energy conformations (Renaud et al., 1995; Klaholz et al., 1998). RXR has an L-shaped pocket, with the longest arm of the pocket shorter than that of RAR. The configuration of the 9–10 double bond in 9cRA generates a retinoid isomer that can easily dock into the L-shaped RXR pocket. By contrast, the extended conformation of atRA would protrude out of the RXR pocket (Figure 4d). Residues C432 and L436 are primarily responsible for the shorter length of the RXR-binding pocket. In RAR, the corresponding residues are glycine and alanine, respectively, which creates a longer binding pocket into which both atRA and 9cRA can fit. The availability of ligand-bound structures for RXR and RAR will aid in the rational design of retinoids with improved selectivity for either receptor.

Binding of Rosiglitazone and GI262570 to PPARγ

The PPARγ ligand-binding site is much larger (~1440 Å^3) and more convoluted than is the corresponding pocket of RXR. Rosiglitazone occupies only 25% of the available pocket. Interestingly, the conformation of rosiglitazone bound to the PPARγ/RXR heterodimer shows significant differences compared with the previously determined rosiglitazone-PPARγ homodimer structure (Nolte et al., 1998). In the heterodimer, rosiglitazone binds into

the large PPARγ pocket in a U-shaped conformation, with the TZD headgroup oriented toward the AF-2 helix (Figure 5). Hydrogen bonds are made between the TZD headgroup and H449, Y473, H323, and S289. However, the hydrogen bond that was seen between the TZD and Q286 in the homodimer structure is absent. The pyridyl tail is directed into a lipophilic pocket adjacent to the β sheet. In the heterodimer, the rosiglitazone side chain adopts a different gauche conformation than it does in the homodimer. In the heterodimer structure, the N-methyl group is directed into a lipophilic pocket between H6 and H7, where it contacts C285, M364, and L353. The pyridyl nitrogen makes a hydrogen bond with a cystallographically observed water molecule within the ligand pocket that was not observed in the homodimer. These differences suggest that heterodimerization has a direct effect on the bound conformation of rosiglitazone.

GI262570 is a tyrosine-based molecule that binds to the PPARγ/RXRα heterodimer with a $K_i = 1$ nM (Henke et al., 1998). This binding affinity is ~50-fold higher than that of rosiglitazone. The X-ray structure of GI262570 in the PPARγ/RXRα heterodimer shows that GI262570 also binds to PPARγ in a U-shaped conformation, occupying ~40% of the pocket (Figure 5b). The carboxyl group of GI262570 makes hydrogen bonds with the same four residues (S289, H323, H449, and Y473) that interacted with the TZD headgroup of rosiglitazone. GI262570 contains a 5-methyl-2-phenyloxazole tail that adopts a gauche conformation, with its methyl group directed into the H6/H7 pocket (Figure 5c). The oxazole nitrogen makes a hydrogen bond with the bound water molecule. As a result, the phenyloxazole tail of GI262570 is inserted ~2.3 Å deeper than is the tail of rosiglitazone into the hydrophobic ligand-binding pocket, while maintaining the critical interactions with the H6/H7 pocket and the bound water molecule (Figure 5). At the other end of GI262570, the benzophenone group attached to the tyrosine nitrogen reaches ~7 Å into a large lipophilic pocket formed by H3, H7, and H10. These hydrophobic interactions, provided by the benzophenone group of GI262570, are not available to rosiglitazone or other TZDs. Thus, the additional hydrophobic interactions of GI262570 with both ends of the ligand-binding pocket reveal the structural basis for its increased PPARγ binding affinity compared with rosiglitazone.

There are several marked differences between the RXRα and PPARγ subunits of the heterodimer with respect to ligand binding. Unlike the enclosed 9cRA-binding pocket in RXR, the PPARγ pocket has a solvent-accessible channel between H3 and the β strands. Rosiglitazone and GI262570 can access the PPARγ pocket via this open channel without the protein undergoing a significant conformational change. Furthermore, rosiglitazone and GI262570 interact directly with the PPARγ AF-2 helix, whereas the RXR AF-2 helix is held in place by 9cRA exclusively through hydrophobic interactions. Thus, ligand binding and activation of PPARγ occur through a mechanism that is distinct from that for RXR. However, the intramolecular interactions between the AF-2 helix and the body of the PPARγ LBD are similar to those seen in the 9cRA/RXR complex. Hydrophobic residues V446, V450, L453, and I456 from H10, together with residues F282, Q286, V290, and V293 from H3 and V322 from H5, form a large hydrophobic pocket for binding of the AF-2 helix. The hydrophobic residues of the AF-2 helix (L468, L469, I472, and Y473) face directly toward this hydrophobic pocket and make extensive interactions with these surrounding residues. The carbonyls of residues 471, 472, and 474 from the PPARγ AF-2 helix are also capped by K319, a conserved positively charged residue from the end of H4. The importance of these capping interactions is underscored by the conservation of these interactions across many nuclear receptors and by the fact that a mutation in the corresponding conserved charged residue in RAR (K264A) abrogates the activity of the receptor (Renaud et al., 1995). These observations demonstrate that although PPARγ ligands interact directly with the AF-2 helix, and RXRα ligands do not, these two receptors employ a conserved set of intramolecular interactions to stabilize the active AF-2 conformation.

Discussion

The RXRs serve as obligate heterodimeric partners for many of the class 1 nuclear receptors, including receptors for atRA, thyroid hormone, vitamin D, eicosanoids, bile acids, and oxysterols (Mangelsdorf and Evans, 1995). As such, the RXRs occupy a pivotal position in vertebrate hormone signaling. We describe two high-resolution crystal structures of liganded PPARγ/RXRα complexes. A striking feature of the heterodimer is its asymmetry where the PPARγ LBD is rotated ~10° from the C2 symmetry axis of the RXR LBD. This differs from the nearly perfect symmetry in the homodimers of the PPARγ and apo-RXRα LBDs (Bourguet et al., 1995; Nolte et al., 1998) and likely accounts for many of the unique properties of heterodimer signaling among nuclear hormone receptors.

Structural Basis for RXR Heterodimerization

Examination of the PPARγ/RXRα heterodimer structure combined with sequence alignments reveals that each of the RXR partners has a consensus heterodimerization motif of $\phi\ \psi K\psi\psi\ \psi K\psi\psi\ \Sigma\ \psi R\psi\psi$ in the first half of H10, where ϕ = the hydrophobic aromatic residues F, W, or Y; ψ = a hydrophobic aliphatic residue with a preference for M, L, V, P, A, or I; and Σ = the acidic residues D or E. The same H10 consensus motif is present in RXR, except for the substitution of A424 at the Σ position. The heterodimer interface is capped at the top of each H10 by the ϕ residue. The remainder of the heterodimer interface consists of mostly hydrophobic interactions between paired ψ residues from the repeating $\psi^{K}/_{R}\psi\psi$ units (Figure 3a). Q, T, and S can substitute for ψ in the second and the third repeating units provided that their side chains are orientated to maximize nonpolar interactions in the dimer interface. This consensus motif is supported by the previous biochemical studies, which showed that mutation of the second $\psi K\psi\psi$ unit in RXR or TR abolished heterodimerization (Zhang et al., 1994; Yang et al., 1996). The basic lysine and arginine residues form salt bridges with conserved glutamic acid and aspartic acid residues in H9 and the 8/9 loop of both receptors. The structures reveal that D441, the Σ residue in the PPARγ dimerization motif, makes an important

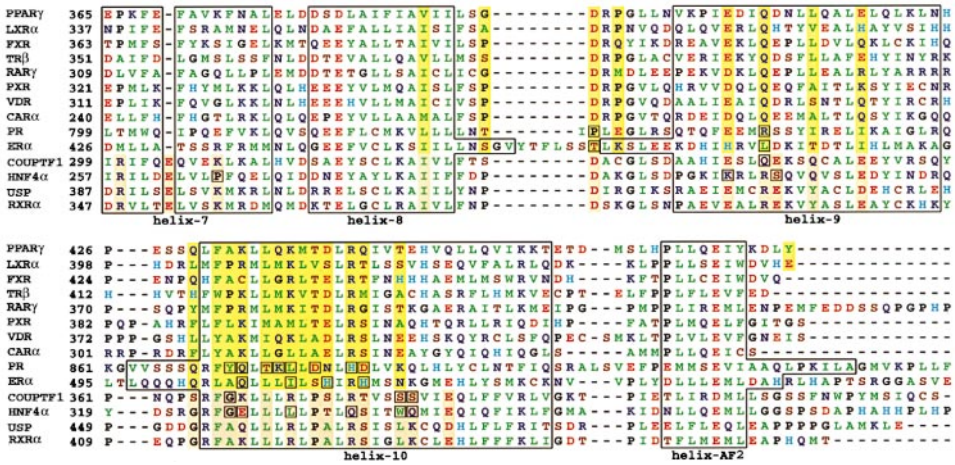

Figure 6. Structure-Based Sequence Alignment of Representative Nuclear Receptors

Only the regions that are involved in the dimerization interface are shown. The PPARγ residues that contact RXR are highlighted in yellow, and the RXRα residues that contact PPARγ are highlighted in orange. The secondary structures are noted under the sequences. The ϕ ψKψψ ψKψψ Σ ψRψψ motif corresponds to the H10 sequences of F AKLL QKMT D LRQI in PPARγ and F AKLL LRLP A LRSI in RXRα. Residues in HNF4, COUPTF1, ERα, and PR that diverge significantly from the consensus motif are boxed. All residues are colored according to their side chain properties (green for hydrophobic, blue for positively charged, red for negatively charged, and brown for polar). Dashes represent gaps in the alignment.

salt bridge with R393 in H9 of RXRα. The reciprocal salt bridge from RXRα to PPARγ cannot form because of the asymmetry of the heterodimer interface (Figure 1), the lack of an acidic Σ residue in H10 of RXRα, and the substitution of Q410R in H9 of PPARγ (Figure 6). The substitutions of A424Σ in RXRα and Q410R in PPARγ, in part, explain the preference of these receptors to form a heterodimers rather than homodimers with themselves (Mangelsdorf and Evans, 1995). The salt bridge between H9 of RXRα and H10 of PPARγ in the heterodimer would be absent in either an RXRα or PPARγ homodimer. This reasoning can be extended to all of the RXR heterodimer partners (Mangelsdorf and Evans, 1995), which each have an Σ residue in the H10 heterodimerization motif and a conserved glutamine residue in H9 (Figure 6). Thus, RXR is uniquely positioned to form heterodimers with its partners, since it is the only mammalian receptor that contains the substitution of both arginine for glutamine in H9 and alanine for the acidic residue in H10. We note that the HNF4 and COUP-TF family members, which are closely related to the RXRs, have several significant variations from the consensus heterodimer motif in H10. This explains why these other subfamily 2 receptors do not function as common heterodimeric partners. Interestingly, however, the *Drosophila* RXR ortholog Ultraspiracle contains both the arginine in H9 and the alanine in H10, which explains its ability to substitute for RXR as a heterodimer partner (Yao et al., 1992; Thomas et al., 1993).

The asymmetry in the major dimerization interface is also reflected in the additional interactions between PPARγ and RXRα, which are important for the preferential formation of the heterodimer relative to either homodimer. The asymmetry of the heterodimer results in the packing of a positively charged region of RXR H7 against a negatively charged surface in PPARγ composed of the end of the AF-2 helix and the 8/9 loop. These interactions are stabilized by a salt bridge between the C-terminal carboxylic acid of PPARγ (Y477) and K431 in H7 of RXRα. The reciprocal salt bridge is unable to form because of the asymmetric nature of the heterodimer interface. The net effect of these additional interactions is to increase the total dimerization interface from approximately 500 Å^2 to 550 Å^2. The preference of PPARγ to form a heterodimer with RXR is thus a consequence of the increased surface contact area as well as charge complementarity at the dimer interface.

An intriguing aspect of RXR heterodimers is that some are permissive for activation by RXR ligands, whereas others are not (Mangelsdorf and Evans, 1995). The PPARγ/RXRα heterodimer falls into the permissive category of RXR heterodimers. Because of the permissive nature of the PPARγ/RXRα heterodimer, RXR agonists have many of the same biological effects as do PPARγ ligands and have been proposed as drugs for the treatment of type 2 diabetes (Mukherjee et al., 1997). The asymmetric interactions between the AF-2 of PPARγ and helices 7 and 10 of RXRα suggest a structural basis for permissiveness. The net effect of these interactions may be the stabilization of the PPARγ AF-2 helix in a position that permits interactions with coactivators, even in the absence of a bound PPARγ agonist. In this configuration, the binding of an agonist in the RXRα side of the heterodimer may result in formation of a second charged clamp, leading to cooperative recruitment of coactivators and activation of transcription. The asymmetric interactions between the PPARγ AF-2 and RXRα may also explain the synergistic activation of the PPARγ/RXRα heterodimer. Binding of a PPARγ agonist holds the AF-2 helix in the active conformation and thus enhances the formation of the functional PPARγ/RXRα heterodimer by stabilizing the interactions between Y477 of PPARγ and helices 7 and 10 of RXRα.

Our model indicates that the salt bridge formed between the C-terminal carboxylate of PPARγ and K431 of RXRα is important for activation of the heterodimer by RXR ligands and allows two predictions. First, disruption of this interaction should prevent activation of the

PPARγ/RXRα heterodimer by 9cRA. In fact, mutations in the PPARγ AF-2 helix that would be expected to severely affect the conformation of the helix result in the loss of heterodimer activation by RXR ligands (Schulman et al., 1998). Notably, mutation of the analogous residues in the RXRα AF-2 results in a heterodimer that can still be activated by rosiglitazone, albeit weakly (Schulman et al., 1998). These findings are consistent with the lack of a corresponding salt bridge between the AF-2 helix of RXRα and helix 7 of PPARγ. A second prediction is that only receptors whose C termini lie at the same position as PPARγ should be permissive for activation by RXR ligands. Alignment of the receptors that heterodimerize with RXR shows that the permissive partners PPARα, PPARδ, LXRα, and LXRβ do indeed truncate at the same position as does PPARγ (Figure 6). FXR, another permissive receptor, is only one residue shorter. RXR may be able to accommodate this one amino acid difference by a slight shift in H7 and H10. The nonpermissive RXR partners RAR, TR, VDR, PXR, and CAR have different length AF-2 tails that could not form the salt bridge with K431 of RXRα. Although this correlation between receptor length and permissiveness for the RXR partners is intriguing, we note that permissiveness will also be regulated at other levels, including the binding of corepressors to receptors, such as the TRs and RARs.

Ligand Activation of RXRα and PPARγ

Comparison of the structure of the apo-RXRα with the structure of the atRA/RAR complex led to the proposal of a mousetrap model of ligand activation (Renaud et al., 1995). This model was based on the observation of an open conformation of the apo-RXR, in which the AF-2 helix is positioned away from the body of the receptor (Bourguet et al., 1995). In all of the agonist-bound nuclear receptor structures, the AF-2 helix is folded against the body of the receptor, generating a hydrophobic cleft into which coactivator proteins can bind (Weatherman et al., 1999). The PPARγ/RXRα structure is consistent with the proposed mousetrap mechanism for the activation of RXR, since the 9cRA/RXRα complex has its AF-2 helix folded against the body of the receptor. However, activation of the nuclear receptor by the mousetrap mechanism may be unique for RXR. RXR has an FFF motif toward the end of H10 that prevents it from forming a stable amphipathic helix. To compensate, the apo-RXRα has a break in H10 that allows F437 and F438, of the FFF motif, to be buried into the hydrophobic core of the receptor. It is this break in H10 that places the C-terminal AF-2 helix in an extended conformation away from the body of the receptor. In the 9cRA/RXRα complex, the β ionone ring of the retinoid fills the hydrophobic pocket that was once occupied by F437 and F438. Thus, the binding of the retinoid ligand results in a large conformational change in RXRα. Most nuclear receptors, including members of subfamily 1, lack the drive to break H10 provided by the FFF motif in RXR. The hydrophobic pocket, into which F437 and F438 are buried in apo-RXR, may also be absent in many of the other receptors. For example, PPARγ places the polar residue H449 in this pocket (Nolte et al., 1998; Uppenberg et al., 1998). This histidine residue is conserved in LXRα, LXRβ, FXR, TR, PXR, and VDR. Therefore, while the PPARγ/RXRα structure supports the mousetrap model for receptor activation for RXR, it also suggests that other nuclear receptors may not require a large conformational change in AF-2 to accommodate their H10 helix. Notably, the apo-PPARγ (Nolte et al., 1998; Uppenberg et al., 1998) and apo-PPARδ (Xu et al., 1999) structures, by contrast with apo-RXR, have their AF-2 helices folded against the body of the receptor in a conformation similar to that of their agonist-bound structures. Thus, there are multiple mechanisms for activating nuclear receptors, even within the single PPARγ/RXRα heterodimeric complex. Ligand-mediated stabilization of the active receptor conformation, without large conformational changes, is likely to be an important paradigm of nuclear receptor activation.

The design of improved drugs to treat type 2 diabetes is an area of intense research in the biomedical community (Willson et al., 2000). Understanding the reciprocal effects of heterodimerization and ligand binding is critically important for the design of drugs that target the PPARγ/RXRα heterodimer. The PPARγ/RXRα crystal structure reveals that heterodimerization can affect ligand binding, since the conformation of rosiglitazone is different in the heterodimer and homodimer complexes. It is also known that rosiglitazone binding to PPARγ can increase heterodimer formation with RXR (Forman et al., 1997). The GI262570-PPARγ/RXRα complex demonstrates how the binding of the lipophilic ligand can be improved by increasing its complementary interactions with the receptor pocket. Thus, the crystal structures of the PPARγ/RXRα heterodimer provide a basis for the rational design of the next generation of drugs for the treatment of type 2 diabetes, and perhaps other diseases.

Since the submission of our paper, the crystal structure of the RAR/RXR heterodimer bound to an RAR antagonist and a fatty acid was published (Bourguet et al., 2000). In this structure, the AF-2 helices of both the RAR and RXR LBDs are folded into the antagonist position; thus, the structure represents an inactive heterodimer. Both of our PPARγ/RXRα heterodimer structures are bound to agonists and coactivator peptides and thus represent the active heterodimer. Comparison of our structures with the RAR/RXR structure reveals that the two heterodimers have a similar dimer interface that is mediated by H7, H9, H10, and the loop between H8 and H9. The consensus heterodimer motif is also present in the RAR LBD (Figure 6); thus, RAR and PPARγ use a similar mechanism for heterodimerization with RXR. However, the asymmetrical character of the PPARγ/RXRα heterodimer was not reported in the RAR/RXR structure, which described a heterodimeric arrangement closely resembling the symmetric homodimers previously reported for the RXRα, ERα, and PPARγ LBD structures (Bourguet et al., 2000). In addition, the RAR/RXR heterodimer is nonpermissive and lacks the asymmetric interactions between the PPARγ AF-2 helix and H7 of RXRα observed here. As discussed above, the asymmetry in the PPARγ/RXRα interface represents a structural basis for the preferential formation of the heterodimer over the respective homodimers. Moreover, the interactions between the PPARγ AF-2 helix and H7

of RXRα may account for the permissive activation of this heterodimer by 9cRA.

Experimental Procedures

Protein Preparation

The RXRα LBD (residues 225–462) was expressed from the T7 promoter of plasmid vector pACYC184, and the PPARγ LBD (residues 206–477 with an N-terminal tag, MKKGHHHHHHG) was expressed from the T7 promoter of plasmid vector pRSET. BL21(DE3) cells transformed with these two expression plasmids were grown in 2YT broth at room temperature to an OD_{600} of ~0.4 and induced with 0.1 mM IPTG for 16 hr. Cells were harvested, resuspended in 250 ml extract buffer (20 mM HEPES [pH 7.5], 25 mM imidozle, and 250 mM NaCl) per 100 g of cells and sonicated for 20 min on ice. The lysate was centrifuged at 40,000 rpm for 40 min, and the supernatant was loaded on a 100 ml Ni-agarose column. The column was washed with 450 ml buffer A (10% glycerol, 20 mM HEPES [pH 7.5], and 25 mM imidizole) and eluted with a 600 ml gradient to 50% buffer B (10% glycerol, 20 mM HEPES [pH 7.5], and 500 mM imidizole). The heterodimer, which eluted at 25% buffer B, was diluted with one volume of buffer C (20 mM HEPES [pH 7.5] and 1 mM EDTA) and loaded on a 100 ml S-Sepharose column. The column was washed with a 100 ml 10% buffer D (20 mM HEPES [pH 7.5], 1 mM EDTA, and 1 M ammonium acetate), and the protein was eluted with a 300 ml gradient to 60% buffer D. The heterodimer complex was eluted at 35% buffer D and was further purified by a second S-Sepharose column. The 1:1 molar ratio of RXRα and PPARγ was confirmed by N-terminal amino acid sequencing and by SDS–PAGE analysis. The final yield of the heterodimer complex was ~17 mg from each liter of cells. The ligand-bound complex was prepared by addition of a 5-fold molar excess of the agnoists and a 3-fold molar excess of the SRC-1 peptide containing the sequence of CPSSHSSLTERHKIL HRLLQEGSPS, followed by filtration and concentration to 10 mg/ml.

Crystallization and Data Collection

Crystals were grown in hanging drops that contained 1 μl of the protein–ligand complex and 1 μl of well buffer that contained 17% PEG 4K, 200 mM NaSCN, 8% ethylene glycol, and 8% glycerol at room temperature. Crystals grew in 1–2 weeks to ~100–500 μm in dimension and diffracted to better than 2.3 Å. Data collections were performed with crystals that were frozen directly from the drops with liquid nitrogen.

The crystals with rosiglitazone formed in space group $P2_1$, with a = 49.1 Å, b = 220.0 Å, c = 55.3 Å, and β = 96.8°. Each asymmetric unit contained two heterodimer complexes with 39% solvent content. The crystals with GI262570 formed in the space group P212121, with a = 46.1 Å, b = 54.1 Å, and c = 211.2 Å. Each asymmetric unit contained one heterodimer complex with 35% of solvent content. Data were collected with a Rigaku R-Axis II detector in house or with a MAR CCD detector in IMCA beamline at the Argonne National Laboratories, and the observed reflections were reduced, merged, and scaled with DENZO and SCALEPACK (Otwinowski et al., 1993) in the HKL2000 package.

Structure Determination and Refinement

The structure was determined by molecular replacement methods with the CCP4 AmoRe program (Collaborative Computational Project Number 4, 1994; Navaza, 1994) using the PPARγ/SRC-1 structure and an active RXR model based on our unpublished 2.0 Å apo-RXR structure (R. T. G. and H. E. X., unpublished data). The solution from the molecular replacement was confirmed by electron density for 9cRA and for the RXR AF-2 helix. Model building was done with quanta, and refinement was progressed with CNS (Brunger et al., 1998) and manual rebuilding. The final model for the 9cRA/rosiglitazone structure includes two heterodimer complexes and 450 water molecules, and has an R factor of 24.2% and free R of 28.8%. The final model for the 9cRA/GI262570 structure includes one heterodimer complex and 133 water molecules, and has an R factor of 23.9% and free R of 26.8%. The statistics of the structures are summarized in Table 1.

Computation

The C2 symmetry axis was calculated as the axis of rotation for the transformation that superimposes the RXRα monomer onto the PPARγ monomer. This superimposition was carried out using 138 Cα atoms selected from the major helices of RXRα and the 138 corresponding Cα atoms in PPARγ. Protein surface areas were calculated with the Connolly MS program, using either the Connnolly molecular surface representation or the alternative solvent-accessible surface representation (Connolly, 1983). Using the Connolly molecular surface, we find that heterodimerization buries 550 $Å^2$, whereas homodimerization only buries 490 $Å^2$ in the PPARγ and 430 $Å^2$ in the RXRα. Using the solvent-accessible surface, we find that heterodimerization buries 1200 $Å^2$ in each monomer, whereas homodimerization buries 1140 $Å^2$ in PPARγ and 1180 $Å^2$ in RXRα. The solvent-accessible surface areas tend to be larger because the surface is displaced 1.4 Å outward from the Van der Waals surface. This displacement may obscure details in the heterodimerization interface, so we prefer the Connolly molecular surface representation.

Acknowledgments

We thank W. Burkart and M. Moyer for protein sequencing, and S. Williams for the initial cells expressing the heterodimer. We would also like to thank R. Nolte and the Industrial Macromolecule Crystallography Association beamline staff at the Argonne National Laboratories for assistance in data collection.

Received February 4, 2000; revised March 2, 2000.

References

Bourguet, W., Ruff, M., Chambon, P., Gronemeyer, H., and Moras, D. (1995). Crystal structure of the ligand-binding domain of the human nuclear receptor RXR-α. Nature *375*, 377–382.

Bourguet, W., Vivat, V., Wurtz, J.-M., Chambon, P., Gronemeyer, H., and Moras, D. (2000). Crystal structure of a heterodimeric complex of RAR and RXR ligand-binding domains. Mol. Cell *5*, 289–298.

Brown, K.K., Henke, B.R., Blanchard, S.G., Cobb, J.E., Mook, R., Kaldor, I., Kliewer, S.A., Lehmann, J.M., Lenhard, J.M., Harrington, W.W., et al. (1999). A novel N-aryl tyrosine activator of peroxisome proliferator-activated receptor-gamma reverses the diabetic phenotype of the Zucker diabetic fatty rat. Diabetes *48*, 1415–1424.

Brunger, A.T., Adams, P.D., Clore, G.M., DeLano, W.L., Gros, P., Grosse-Kunstleve, R.W., Jiang, J.S., Kuszewski, J., Nilges, M., Pannu, N.S., et al. (1998). Crystallography and NMR system: a new software suite for macromolecular structure determination. Acta Crystallogr. D Biol. Crystallogr. *54*, 905–921.

Brzozowski, A.M., Pike, A.C.W., Dauter, Z., Hubbard, R.E., Bonn, T., Engstrom, O., Ohman, L., Greene, G.L., Gustafsson, J.-A., and Carlquist, M. (1997). Molecular basis of agonism and antagonism in the oestrogen receptor. Nature *389*, 753–758.

Collaborative Computational Project Number 4 (1994). The CCP4 suite: programs for protein crystallography. Acta Crystallogr. D *50*, 760–776.

Connolly, M.L. (1983). Solvent-accessible surfaces of proteins and nucleic acids. Science *221*, 709–713.

Forman, B.M., Chen, J., and Evans, R.M. (1997). Hypolipidemic drugs, polyunsaturated fatty acids, and eicosanoids are ligands for peroxisome proliferator-activated receptors α and δ. Proc. Natl. Acad. Sci. USA *94*, 4312–4317.

Freedman, L.P. (1999). Increasing the complexity of coactivation in nuclear receptor signaling. Cell *97*, 5–8.

Henke, B.R., Blanchard, S.G., Brackeen, M.F., Brown, K.K., Cobb, J.E., Collins, J.L., Harrington, W.W., Jr., Hashim, M.A., Hull-Ryde, E.A., Kaldor, I., et al. (1998). N-(2-Benzoylphenyl)-L-tyrosine PPARγ agonists. I. Discovery of a novel series of potent antihyperglycemic and antihyperlipidemic agents. J. Med. Chem. *41*, 5020–5036.

Heyman, R.A., Mangelsdorf, D.J., Dyck, J.A., Stein, R., Eichele, G., Evans, R.M., and Thaller, C. (1992). 9-cis retinoic acid is a high affinity ligand for the retinoid X receptor. Cell *68*, 397–406.

Klaholz, B.P., Renaud, J.P., Mitschler, A., Zusi, C., Chambon, P., Gronemeyer, H., and Moras, D. (1998). Conformational adaptation of agonists to the human nuclear receptor RARγ. Nat. Struct. Biol. *5*, 199–202.

Kliewer, S.A., Forman, B.M., Blumber, B., Ong, E.S., Borgmeyer, U., Mangelsdorf, D.J., Umesono, K., and Evans, R.M. (1994). Differential expression and activation of a family of murine peroxisome proliferator-activated receptors. Proc. Natl. Acad. Sci. USA *91*, 7355–7359.

Kliewer, S.A., and Willson, T.M. (1998). The nuclear receptor PPARγ—bigger than fat. Curr. Opin. Genet. Dev. *8*, 576–581.

Levin, A.A., Sturzenbecker, L.J., Kazmer, S., Bosakowski, T., Huselton, C., Allenby, G., Speck, J., Kratzeisen, C., Rosenberger, M., Lovey, A., et al. (1992). 9-cis retinoic acid stereoisomer binds and activates the nuclear receptor RXRα. Nature *355*, 359–361.

Mangelsdorf, D.J., and Evans, R.M. (1995). The RXR heterodimers and orphan receptors. Cell *83*, 841–850.

Mukherjee, R., Davies, P.J.A., Crombie, D.L., Bischoff, E.D., Cesario, R.M., Jow, L., Hamann, L.G., Boehm, M.F., Mondon, C.E., Nadzan, A.M., et al. (1997). Sensitization of diabetic and obese mice to insulin by retinoid X receptor agonists. Nature *386*, 407–410.

Navaza, J. (1994). AmoRe: an automated package for molecular replacement. Acta Crystallogr. A *50*, 157–163.

Nolte, R.T., Wisely, G.B., Westin, S., Cobb, J.E., Lambert, M.H., Kurokawa, R., Rosenfeld, M.G., Willson, T.M., Glass, C.K., and Milburn, M.V. (1998). Ligand binding and co-activator assembly of the peroxisome proliferator-activated receptor-γ. Nature *395*, 137–143.

Nuclear Receptors Nomenclature Committee (1999). A unified nomenclature system for the nuclear receptor superfamily. Cell *97*, 161–163.

Otwinowski, Z., Isaacs, N., and Burley, S. (1993). Oscillation data reduction program. In Proceedings of the CCP4 Study Weekend, L. Sawyer, ed. (Daresbury, UK: SERC Daresbury Laboratory), pp. 56–62.

Peet, D.J., Doyle, D.F., Corey, D.R., and Mangelsdorf, D.J. (1998). Engineering novel specificities for ligand-activated transcription in the nuclear hormone receptor RXR. Chem. Biol. *5*, 13–21.

Renaud, J.-P., Rochel, N., Ruff, M., Vivat, V., Chambon, P., and Moras, D. (1995). Crystal structure of the RAR-γ ligand-binding domain bound to all-trans retinoic acid. Nature *378*, 681–689.

Schoonjans, K., Martin, G., Staels, B., and Auwerx, J. (1997). Peroxisome proliferator-activated receptors, orphans with ligands and functions. Curr. Opin. Lipidol. *8*, 159–166.

Schulman, I.G., Shao, G., and Heyman, R.A. (1998). Transactivation by retinoid X receptor–peroxisome proliferator-activated receptor γ (PPARγ) heterodimers: intermolecular synergy requires only the PPARγ hormone–dependent activation function. Mol. Cell. Biol. *18*, 3483–3494.

Shiau, A.K., Barstad, D., Loria, P.M., Cheng, L., Kushner, P.J., Agard, D.A., and Greene, G.L. (1998). The structural basis of estrogen receptor/coactivator recognition and the antagonism of this interaction by tamoxifen. Cell *95*, 927–937.

Spiegelman, B.M. (1998). PPAR-γ: adipogenic regulator and thiazolidinedione receptor. Diabetes *47*, 507–514.

Thomas, H.E., Stunnenberg, H.G., and Stewart, A.F. (1993). Heterodimerization of the Drosophila ecdysone receptor with retinoid X receptor and ultraspiracle. Nature *362*, 471–475.

Tontonoz, P., Graves, R.A., Budvari, A.I., Erdjument-Bromage, H., Lui, M., Hu, E., Tempst, P., and Spiegelman, B.M. (1994). Adipocyte-specific transcription factor ARF6 is a heterodimeric complex of two nuclear hormone receptors, PPARgamma and RXRalpha. Nucl. Acids Res. *22*, 5628–5634.

Uppenberg, J., Svensson, C., Jaki, M., Bertilsson, G., Jendeberg, L., and Berkenstam, A. (1998). Crystal structure of the ligand binding domain of the human nuclear receptor PPARγ. J. Biol. Chem. *273*, 31108–31112.

Wagner, R.L., Apriletti, J.W., McGrath, M.E., West, B.L., Baxter, J.D., and Fletterick, R.J. (1995). A structural role for hormone in the thyroid hormone receptor. Nature *378*, 690–697.

Weatherman, R.V., Fletterick, R.J., and Scanlan, T.S. (1999). Nuclear-receptor ligands and ligand-binding domains. Annu. Rev. Biochem. *68*, 559–581.

Williams, S.P., and Sigler, P.B. (1998). Atomic structure of progesterone complexed with its receptor. Nature *393*, 392–396.

Willson, T.M., and Wahli, W. (1997). Peroxisome proliferator-activated receptor agonists. Curr. Opin. Chem. Biol. *1*, 235–241.

Willson, T.M., Brown, P.J., Sternbach, D.D., and Henke, B.R. (2000). The PPARs: from orphan receptors to drug discovery. J. Med. Chem. *43*, 527–550.

Wurtz, J.-M., Bourguet, W., Renaud, J.-P., Vivat, V., Chambon, P., Moras, D., and Gronemeyer, H. (1996). A canonical structure for the ligand-binding domain of nuclear receptors. Nat. Struct. Biol. *3*, 87–94.

Xu, H.E., Lambert, M.H., Montana, V.G., Parks, D.J., Blanchard, S.G., Brown, P.J., Sternbach, D.D., Lehmann, J.M., Wisely, G.B., Willson, T.M., et al. (1999). Molecular recognition of fatty acids by peroxisome proliferator-activated receptors. Mol. Cell *3*, 397–403.

Yang, Y.Z., Burgos-Trinidad, M., Wu, Y., and Koenig, R.J. (1996). Thyroid hormone receptor variant alpha2. Role of the ninth heptad in DNA binding, heterodimerization with retinoid X receptors, and dominant negative activity. J. Biol. Chem. *271*, 28235–28242.

Yao, T.P., Segraves, W.A., Oro, A.E., McKeown, M., and Evans, R.M. (1992). Drosophila ultraspiracle modulates ecdysone receptor function via heterodimer formation. Cell *71*, 63–72.

Zhang, X.K., Salbert, G., Lee, M.O., and Pfahl, M. (1994). Mutations that alter ligand-induced switches and dimerization activities in the retinoid X receptor. Mol. Cell. Biol. *14*, 4311–4323.